MATHEMATICAL MODELING AND COMPUTING, Vol. 9, No. 3, pp. 663–677 (2022)

Retrieving the Robin coefficient from single Cauchy data in elliptic systems

El Madkouri A., Ellabib A.

Faculty of Sciences and Techniques,
Department of Mathematics and Informatics LAMAI,
Cadi Ayyad University, Marrakech, Morocco

(Received 16 February 2022; Revised 4 July 2022; Accepted 5 July 2022)

The purpose of this work is to identify a Robin coefficient from available measurements on the accessible part of the boundary. After recasting the inverse problem as an optimization problem, we study the issue of identifiability, stability, and identification. For the reconstruction process, two regularized algorithms are designed, and the forward problem is approximated using the discontinuous dual reciprocity method. The accuracy of the proposed approaches is tested in the case of noise–free and noisy data and the findings are very promising and encouraging.

Keywords: *boundary element method, discontinuous reciprocity approximation, Levenberg–Marquardt algorithm, quasi–Newton algorithms, Robin parameter reconstruction.*

2010 MSC: 65N38, 65M38, 90C53, 65M32, 45Q05 **DOI:** 10.23939/mmc2022.03.663

1. Introduction

In this work, we consider the inverse problem of identifying a Robin coefficient of a 2D elliptic equation for anisotropic inhomogeneous media using some partial boundary measurements. This type of ill-posed problem has received much attention over the last three decades, both from theoretical and numerical aspects. The inverse Robin problem arises naturally in many physical situations, a rather incomplete list of such applications may be found in terms of estimation of parameters in thermal models [1, 2], corrosion detection of an electrostatic conductor [3,4], the metal-silicon contact in MOSFET devices [5], quenching processes [6], we refer to [7] and the references therein for more engineering applications.

All these applications usually lead to estimating the Robin coefficient on an inaccessible boundary from additional data, which are supposed to be either internal or on the accessible part of the boundary. Such measurements are usually contaminated with noise, which complicates the recovery process; in other words, the compatibility condition is not guaranteed to ensure the existence of a solution, and any small error in the data may lead to an erroneous solution; therefore, one needs to solve the problem in a different way equivalent to the original problem.

Generally speaking, during the reconstruction process of the Robin coefficient, one has to investigate three major issues: uniqueness, stability, and identification. Regarding the uniqueness of the Robin parameter, in [3] the author proved that the Robin parameter can be uniquely determined via some boundary measurements assuming a specific regularity on the yet unknown coefficient ($C^3(\partial\Omega)$ with $\partial\Omega$ is the boundary of the domain problem), the result was then extended in [8] to the case of continuous Robin coefficient with some restriction on the boundedness of the parameter, whereas Choulli [9] has proved some results for the non-linear heat equation. In numerical applications, the stability is very important criterion, one has to ensure the continuous dependence of the unknown parameter on the additional data, in this context we may cite the work of [8] who has established a local and directional Lipschitz stability estimate, Choulli [9] has proved a local Lipschitz stability estimate for an arbitrary smooth domain and a log-log stability estimate for rectangular domains, whereas Sincich [10] developed a global Lipschitz stability estimate of sparse Robin coefficient, however, the Lipschitz

constant explodes exponentially as the Robin coefficient tends to infinity. In particular, the logarithmic global stability of the Robin inverse problem has been well established by many authors, the reader may consult the references [9, 11–14] and the references therein. Regarding the identification issue, many numerical methods were proposed, among them, we may cite the work of [15] who used an iterative gradient process by minimizing a trace error, in [16] the authors proposed to minimize the difference between the outside and inside temperature on the accessible part of the boundary, a thin plate approximation of the Robin coefficient was adopted in [3], whereas in [17] a minimization procedure based on a trigonometric polynomial approximation is studied.

In the present work, we are concerned with a nonlinear inverse Robin problem associated with a general elliptic equation for inhomogeneous anisotropic materials from additional boundary data. The problem is transformed into an optimization one and the forward problem is approximated using the discontinuous dual reciprocity boundary element method, whereas two automated regularizing algorithms are presented and used to stably recover the unknown Robin coefficient. The discontinuous dual reciprocity method in conjuncture with regularized quasi-Newton algorithm was established by the authors for the case of inverse source problem, see [18–20].

The rest of the work is organized as follows, in the second section, the forward and inverse models are outlined, and an equivalent formulation of the initial inverse problem is also established. In section 3, the inverse Robin problem is analyzed, the numerical approximation of the forward model as well as the proposed algorithms are described in the section 4, numerical validations are investigated in section 5. Our conclusions are drawn in the final section.

2. Model problems

The purpose of this section is to introduce and state the direct and inverse problems. The first part is concerned with the presentation of the direct problem then a well-posedness result is stated, next we describe the mathematical formulation of the Robin inverse problem.

2.1. Forward model problem

We consider here the following mixed boundary value problem for anisotropic inhomogeneous materials, let Ω be a bounded connected domain in $\mathbb{R}^2$, its boundary $\Gamma = \partial\Omega$ is a simple closed curve such that $\Gamma = \Gamma_N \cup \Gamma_R$ with $\Gamma_N \cap \Gamma_R = \varnothing$:

$$\begin{cases} -\nabla \cdot (\xi(\mathrm{x})\nabla u) + b(\mathrm{x})u = f(\mathrm{x}) & \text{in } \Omega, \\ \xi(\mathrm{x})\dfrac{\partial u}{\partial n} = h(\mathrm{x}) & \text{on } \Gamma_N, \\ \xi(\mathrm{x})\dfrac{\partial u}{\partial n} + \gamma(\mathrm{x})u(\mathrm{x}) = k(\mathrm{x}) & \text{on } \Gamma_R. \end{cases} \tag{1}$$

The coefficients $\xi(\mathrm{x})$ and $b(\mathrm{x})$ can be viewed, respectively, as the heat conductivity and radiation, which satisfy the conditions: $0 < \xi_0 \leqslant \xi(\mathrm{x}) \leqslant \xi_1$, $0 \leqslant b_0 \leqslant b(\mathrm{x}) \leqslant b_1$, whereas the function $f(\mathrm{x})$ may model the source strength and $k(\mathrm{x})$ is the ambient temperature.

The following lemma states that the forward problem (1) is well posed.

Lemma 1 (see Lions and Magenes [21]). *Let Ω be an open bounded and connected domain with C^1 boundary, $\xi(\mathrm{x}) \in H^1(\Omega)$, $b(\mathrm{x}) \in L^\infty(\Omega)$, and $\gamma(\mathrm{x}) \in L^\infty(\Gamma_R)$ with positive lower and upper bounds ξ_0, ξ_1, b_0, b_1 and γ_1, γ_2, respectively, then there exists a unique solution $u \in H^1(\Omega)$ of the system (1).*

2.2. Inverse model problem formulation and uniqueness result

As stated previously, our main interest is to recover the Robin parameter $\gamma(\mathrm{x})$ lying in the inaccessible part Γ_R. Therefore, we need some extra measurements of the solution of the forward model (1), in

this work, the measurements are supposed to be available on the accessible boundary Γ_N. Roughly speaking, the inverse Robin problem is given as follows.

Inverse Robin problem: Recover the coefficient γ on Γ_R through the measurement data $\tilde{u}$ of u on Γ_N.

In the following, we establish an identifiability result, and we prove that the inverse Robin problem is uniquely determined by the additional data of u on Γ_N. We have the following theorem.

Theorem 1 (Uniqueness). *Let η_1 and η_2 be two solutions of the inverse problem (5), we assume that the boundary $\partial\Omega$ is smooth enough,* $\text{meas}\{x \in \Gamma_R \colon u(\eta_1) = 0\} = 0$ *and $u(\eta_1) = u(\eta_2)$ on Γ_N, then $\eta_1 = \eta_2$ a.e. on Γ_R.*

Proof. Let us denote $\omega = u(\eta_1) - u(\eta_2)$, with $\eta_1, \eta_2 \in \gamma_{ad}$ such that $u(\eta_1) = u(\eta_2)$ on Γ_N.

We can easily verify that ω solves the following problem:

$$\begin{aligned} -\nabla \cdot (\xi(\mathbf{x})\nabla\omega) + b(\mathbf{x})\omega = 0 \quad &\text{in } \Omega, \\ \xi(\mathbf{x})\frac{\partial\omega}{\partial n} = 0 \quad &\text{on } \Gamma_N, \\ \omega = 0 \quad &\text{on } \Gamma_N. \end{aligned}$$

By applying the unique continuation principle [22], we have $\omega = 0$ in Ω, hence, by the trace theorem, we have $\omega = 0$ on $\partial\Omega$.

On the other hand, we have on Γ_R

$$\xi(\mathbf{x})\frac{\partial\omega}{\partial n} + \eta_1 u\,(\eta_1) - \eta_2 u\,(\eta_2) = 0,$$

thus we have

$$u(\eta_1)(\eta_1 - \eta_2) = 0 \quad \text{a.e. on } \Gamma_R.$$

Since $\text{meas}\{x \in \Gamma_R \colon u(\eta_1) = 0\} = 0$ we obtain $\eta_1 = \eta_2$ a.e. on Γ_R. ∎

3. Analysis of the inverse Robin problem

We note that in real-life applications, the measurement data are always contaminated with noise. We assume that the noise level of the observation data $\tilde{u}_\delta$ of the true solution $\tilde{u}$ is of the order δ, such that

$$\|\tilde{u}_\delta - \tilde{u}\|_{L^2(\Gamma_N)} \leqslant \delta.$$

Since the inverse problem is known to be ill-posed, a stabilization technique is needed. In this paper, we formulate the inverse Robin problem as a stabilized nonlinear minimization problem with the standard Tikhonov regularization:

$$\min_{\gamma \in \gamma_{ad}} J(u, \gamma) := \frac{1}{2}\int_{\Gamma_N} (u(\gamma) - \tilde{u}_\delta)^2 ds + \alpha \int_{\Gamma_R} \gamma^2 ds, \tag{2}$$

with

$$\gamma_{ad} = \{\gamma(\mathrm{x}) \in L^\infty(\Gamma_R) \colon 0 < \gamma_1 \leqslant \gamma \leqslant \gamma_2 \text{ a.e. on } \Gamma_R\},$$

and $u(\gamma) \in H^1(\Omega)$ is the solution of the forward problem which satisfying:

$$\int_\Omega \xi \nabla u \cdot \nabla\phi\, dx + \int_\Omega bu\phi\, dx + \int_{\Gamma_R} \gamma u\phi\, ds = \int_\Omega f\phi\, dx + \int_{\Gamma_R} k\phi\, ds + \int_{\Gamma_N} h\phi\, ds \quad \forall \phi \in H^1(\Omega). \tag{3}$$

We introduce the coefficient to solution map named $\mathbb{F}$ given as follows:

$$\begin{aligned}\mathbb{F}\colon \gamma_{ad} &\longmapsto L^2(\Gamma_N),\\ \gamma &\longmapsto \mathbb{F}(\gamma) := u(\gamma).\end{aligned}$$

The optimization problem (2) can now be reduced as:

$$\min_{\gamma\in\gamma_{ad}} J(\gamma) := \frac{1}{2}\int_{\Gamma_N}(\mathbb{F}(\gamma)-\tilde{u}_\delta)^2 ds + \alpha\int_{\Gamma_R}\gamma^2 ds. \tag{4}$$

The inverse Robin problem is now formulated as follows:

$$\text{Find}\quad \gamma^*\in\gamma_{ad}\ \text{ s.t: }\ J(\gamma^*)\leqslant J(\gamma)\quad \forall\gamma\in\gamma_{ad}\ \text{ and }\ u(\gamma)\ \text{ solves }\ (3). \tag{5}$$

In order to take into account the instabilities of the inverse Robin problem caused by the noise in the additional data, the problem is formulated by a constrained optimization problem given in (5), the aim now is to prove that the minimization problem has at least one solution.

Theorem 2. *The optimization problem (5) admits at least one solution.*

Proof. It is straightforward to see that $\inf J(\gamma)$ is finite over the admissible set γ_{ad}, hence there exists a minimizing sequence denoted $\gamma_n\in\gamma_{ad}$ such that

$$\lim_{n\to\infty} J(\gamma_n) = \inf_{\gamma\in\gamma_{ad}} J(\gamma).$$

The boundedness of γ_n in γ_{ad} ensures the existence of a subsequence still denoted γ_n such that γ_n converges weakly $*$ to some γ^* in $L^\infty(\Gamma_R)$ where in particular we have used Banach–Alaoglu theorem. Next we prove that γ^* is a minimizer of (5).

We let $u_n = u(\gamma_n)$, hence it satisfies the variational form (3):

$$\int_\Omega \xi\nabla u_n\cdot\nabla\phi\,dx + \int_\Omega b u_n\phi\,dx + \int_{\Gamma_R}\gamma u_n\phi\,ds = \int_\Omega f\phi\,dx + \int_{\Gamma_R} k\phi\,ds + \int_{\Gamma_N} h\phi\,ds\quad \forall\phi\in H^1(\Omega).$$

We can easily derive the following inequality

$$\begin{aligned}\min\{\xi_0,b_0\}\|u_n\|^2_{H^1(\Omega)} &+ \gamma_1\|u_n\|^2_{L^2(\Gamma_R)}\\ &\leqslant \|f\|_{L^2(\Omega)}\|u_n\|_{L^2(\Omega)} + \|k\|_{L^2(\Gamma_R)}\|u_n\|_{L^2(\Gamma_R)} + \|h\|_{L^2(\Gamma_N)}\|u_n\|_{L^2(\Gamma_N)}\\ &\leqslant C\left(\|f\|_{L^2(\Omega)} + \|k\|_{L^2(\Gamma_R)} + \|h\|_{L^2(\Gamma_N)}\right)\|u_n\|_{H^1(\Omega)} \leqslant C\|u_n\|_{H^1(\Omega)},\end{aligned}$$

where we take $\phi = u_n$ and we use the fact that $\|u_n\|_{L^2(\partial\Omega)}\leqslant C\|u_n\|_{H^1(\Omega)}$ (the trace theorem) and the boundedness of ξ, b and γ_n. Consequently, there exists a constant $C\geqslant 0$ independent of n such that: $\|u_n\|_{H^1(\Omega)}\leqslant C$, hence there exists a subsequence still denoted u_n and some $u^*\in H^1(\Omega)$ such that $u_n\rightharpoonup u^*$, by using the continuous embedding of $H^1(\Omega)$ in $H^{1/2}(\partial\Omega)$ (trace theorem) and the compact embedding of $H^{1/2}(\partial\Omega)$ in $L^2(\Omega)$ we deduce the strong convergence of $u_n\to u^*$ in $L^2(\partial\Omega)$.

Next we prove that $u^* = u(\gamma^*)$, we have for every $\phi\in H^1(\Omega)$:

$$\int_{\Gamma_R}\gamma_n u_n\phi\,ds = \int_{\Gamma_R}\gamma_n(u_n-u^*)\phi\,ds + \int_{\Gamma_R}\gamma_n u^*\phi\,ds$$

using the boundedness of γ_n, the strong convergence of u_n in $L^2(\partial\Omega)$ and the weak convergence of γ_n, we conclude that:

$$\lim_{n\to\infty}\int_{\Gamma_R}\gamma_n u_n\phi\,ds = \int_{\Gamma_R}\gamma^* u^*\phi\,ds.$$

Since u_n verifies for every $\phi \in H^1(\Omega)$

$$\int_\Omega \xi \nabla u_n \cdot \nabla \phi \, dx + \int_\Omega b u_n \phi \, dx + \int_{\Gamma_R} \gamma_n u_n \phi \, ds = \int_\Omega f \phi \, dx + \int_{\Gamma_R} k \phi \, ds + \int_{\Gamma_N} h \phi \, ds \quad \forall \phi \in H^1(\Omega).$$

We thus have by letting $n \to \infty$:

$$\int_\Omega \xi \nabla u^* \cdot \nabla \phi \, dx + \int_\Omega b u^* \phi \, dx + \int_{\Gamma_R} \gamma^* u^* \phi \, ds = \int_\Omega f \phi \, dx + \int_{\Gamma_R} k \phi \, ds + \int_{\Gamma_N} h \phi \, ds \quad \forall \phi \in H^1(\Omega).$$

From which we conclude that $u^* = u(\gamma^*)$.

By using the fact that:

$$\lim_{n\to\infty} \int_{\Gamma_N} (\mathbb{F}(\gamma_n) - \tilde{u}_\delta)^2 ds = \int_{\Gamma_N} (\mathbb{F}(\gamma^*) - \tilde{u}_\delta)^2 ds$$

and the lower semi-continuity of a norm we get:

$$\begin{aligned} J(\gamma^*) &= \|\mathbb{F}(\gamma^*) - \tilde{u}_\delta\|^2_{\Gamma_N} + \alpha \|\gamma^*\|^2_{\Gamma_R} \\ &= \lim_{n\to\infty} \|\mathbb{F}(\gamma_n) - \tilde{u}_\delta\|^2_{\Gamma_N} + \alpha \|\gamma^*\|^2_{\Gamma_R} \\ &\leqslant \lim_{n\to\infty} \|\mathbb{F}(\gamma_n) - \tilde{u}_\delta\|^2_{\Gamma_N} + \alpha \liminf_{n\to\infty} \|\gamma_n\|^2_{\Gamma_R} \\ &\leqslant \liminf_{n\to\infty} J(\gamma_n) = \inf_{\gamma\in\gamma_{ad}} J(\gamma). \end{aligned}$$

Hence γ^* is a minimizer of (5). ∎

We shall now prove that the formulation (5) is stable with respect to the noise in the measurement data.

Theorem 3. *Let $\tilde{u}^n_\delta$ be a sequence such that $\tilde{u}^n_\delta \to \tilde{u}_\delta$ in $L^2(\Gamma_N)$, we let also $\gamma^n \in \gamma_{ad}$ such that $J(\gamma^n) = \inf_{\gamma\in\gamma_{ad}} J(\gamma)$ is the solution to the optimization problem with $\tilde{u}_\delta$ replaced by $\tilde{u}^n_\delta$. Thus, we have the existence of a subsequence of γ^n that converges weakly $*$ in $L^\infty(\Gamma_R)$ to the minimizer of (5).*

Proof. By definition, the sequence γ^n admits a subsequence still denoted γ^n and there exists $\gamma^* \in \gamma_{ad}$ such that

$$\gamma^n \to \gamma^* \quad \text{in } L^\infty(\Gamma_R) \text{ weakly } *.$$

Similarly as was done in theorem (2), we can deduce the following convergences:

$$\begin{aligned} &u(\gamma^n) \to u(\gamma^*) \text{ weakly in } H^1(\Omega), \\ &\mathbb{F}(\gamma^n) \to \mathbb{F}(\gamma^*) \text{ strongly in } L^2(\Gamma_N). \end{aligned}$$

By using the strong convergence $\tilde{u}^n_\delta \to \tilde{u}_\delta$ in $L^2(\Gamma_N)$ and $\mathbb{F}(\gamma^n) \to \mathbb{F}(\gamma^*)$ in $L^2(\Gamma_N)$, we can then derive the following:

$$\begin{aligned} J(\gamma^*) &= \frac{1}{2} \int_{\Gamma_N} (\mathbb{F}(\gamma^*) - \tilde{u}_\delta)^2 \, ds + \alpha \int_{\Gamma_R} (\gamma^*)^2 ds \\ &\leqslant \lim_{n\to\infty} \frac{1}{2} \int_{\Gamma_N} \mathbb{F}(\gamma^n - \tilde{u}^n_\delta)^2 ds + \lim_{n\to\infty} \inf \alpha \int_{\Gamma_R} (\gamma^n)^2 ds \\ &\leqslant \lim_{n\mapsto\infty} \inf \left(\frac{1}{2} \int_{\Gamma_N} (\mathbb{F}(\gamma^n) - \tilde{u}^n_\delta)^2 \, ds + \alpha \int_{\Gamma_R} (\gamma^n)^2 ds \right) \\ &= \frac{1}{2} \int_{\Gamma_N} (\mathbb{F}(\gamma) - \tilde{u}_\delta)^2 ds + \alpha \int_{\Gamma_R} \gamma^2 ds = J(\gamma). \end{aligned}$$

Which completes the proof. ∎

4. Numerical formulation

In this part, we focus on the approximation of the forward model using a discontinuous dual reciprocity boundary element method, this is a fundamental step in the resolution of the inverse model, where the optimization problem (5) involves the resolution of the forward problem for a given Robin parameter γ. We propose a gradient-type algorithm for the nonlinear optimization problem, which takes into account the measurement errors.

4.1. Approximation of the forward model

The boundary element method is an important technique in engineering analysis, it reduces the dimensionality of the investigated problem by one; thus, it reduces the amount of data needed to solve a problem, however, it loses its advantage of boundary discretization only. When it is applied to nonlinear, non-homogeneous and transient problems, the domain integral appears in the resulting integral equations, the dual reciprocity method [23] can overcome this drawback by taking the domain integral to the boundary [24, 25]. In this paper, a discontinuous dual reciprocity boundary element method is adopted to solve the direct problem.

We shall begin by the following substitution

$$u(x,y) = \frac{1}{\sqrt{\xi(x,y)}} w(x,y). \tag{6}$$

We find that (16) can be re-written as

$$-\Delta w + \left(\frac{\gamma(x,y)}{\sqrt{\xi(x,y)}} + p(x,y) \right) w = \frac{1}{\sqrt{\xi(x,y)}} f(x,y),$$

where

$$p(x,y) = \frac{1}{\sqrt{\xi(x,y)}} \Delta(\sqrt{\xi(x,y)}).$$

The partial differential equation may be used to derive the integral equation, from classical analysis, the solution w can be represented by boundary potentials as follows:

$$\begin{aligned} \lambda(\xi,\eta) w(\xi,\eta) = & \int_\Omega w^*(x,y;\xi,\eta) \left[\left[\frac{b(x,y)}{\sqrt{\xi(x,y)}} + p(x,y) \right] w(x,y) - \frac{1}{\sqrt{\xi(x,y)}} f(x,y) \right] dx\, dy \\ & + \int_{\partial\Omega} \left[w(x,y) \frac{\partial w^*}{\partial n}(x,y;\xi,\eta) - u^*(x,y;\xi,\eta) \frac{\partial w(x,y)}{\partial n} \right] ds. \end{aligned} \tag{7}$$

Where

$$\lambda(\xi,\eta) \;=\; \begin{cases} 1, & \text{if } (\xi,\eta) \in \Omega; \\ 1/2, & \text{if } (\xi,\eta) \in \partial\Omega; \\ 0, & \text{if not;} \end{cases}$$

and

$$w^*(x,y;\xi,\eta) = \frac{1}{2\pi} \ln \sqrt{(x-\xi)^2 + (y-\eta)^2}, \quad \frac{\partial w^*}{\partial n}(x,y;\xi,\eta) = \frac{1}{2\pi} \frac{(x-\xi) n_1(x,y) + (y-\eta) n_2(x,y)}{(x-\xi)^2 + (y-\eta)^2}.$$

For the dual reciprocity boundary element method, the boundary $\partial\Omega$ is discretized into N straight line elements $E^{(m)}$, the starting and ending points of the boundary element $E^{(m)}$ are given by $(a_1^{(m)}, a_2^{(m)})$ and $(b_1^{(m)}, b_2^{(m)})$ respectively. For an accurate approximation, w and $\frac{\partial w}{\partial n}$ are approximated using discontinuous linear boundary elements.

Two points $(x_1^{(m)}, x_2^{(m)})$ and $(x_1^{(N+m)}, x_2^{(N+m)})$ on $E^{(m)}$ are chosen as follows:

$$\begin{cases} x_i^{(m)} = a_i^{(m)} + r(b_i^{(m)} - a_i^{(m)}), \\ x_i^{(N+m)} = b_i^{(m)} - r(b_i^{(m)} - a_i^{(m)}), \end{cases} \quad \text{for} \quad r \in \left(0, \tfrac{1}{2}\right)$$

If w has values $w^{(m)}$ and $w^{(N+m)}$ at $(x_1^{(m)}, x_2^{(m)})$ and $(x_1^{(N+m)}, x_2^{(N+m)})$, respectively, then one makes the approximation:

$$w(x,y) \simeq \left[1 - r^{(m)}(x,y)\right] w^{(m)} + r^{(m)}(x,y) w^{(N+m)}, \tag{8}$$

where

$$r^{(m)}(x,y) = \frac{\sqrt{(x - a_1^{(m)})^2 + (y - a_2^{(m)})^2} - r l^{(m)}}{(1-2r) l^{(m)}}.$$

Similarly for the flux.

From (8), (7) approximately becomes

$$\begin{aligned} \lambda(\xi,\eta) w(\xi,\eta) = & \int_\Omega w^*(x,y;\xi,\eta) \left[[\frac{b(x,y)}{\sqrt{\xi(x,y)}} + p(x,y)] w(x,y) - f(x,y) \right] dx\, dy \\ & + \sum_{m=1}^{N} w^{(m)} I_1^{(m)}(\xi,\eta) \; + \; w^{(N+m)} I_3^{(m)}(\xi,\eta) \\ & - \frac{\partial w^{(m)}}{\partial n} I_2^{(m)}(\xi,\eta) - \frac{\partial w(x,y)}{\partial n} I_4^{(m)}(\xi,\eta), \end{aligned} \tag{9}$$

where

$$\begin{aligned} I_1^{(m)}(\xi,\eta) &= \int_{E^{(m)}} (1 - r^{(m)}) \frac{\partial u^*}{\partial n}(x,y;\xi,\eta)\, ds(x,y), \\ I_2^{(m)}(\xi,\eta) &= \int_{E^{(m)}} (1 - r^{(m)}) u^*(x,y;\xi,\eta)\, ds(x,y), \\ I_3^{(m)}(\xi,\eta) &= \int_{E^{(m)}} r^{(m)} \frac{\partial u^*}{\partial n}(x,y;\xi,\eta)\, ds(x,y), \\ I_4^{(m)}(\xi,\eta) &= \int_{E^{(m)}} r^{(m)} u^*(x,y;\xi,\eta)\, ds(x,y). \end{aligned}$$

To deal with the domain integral in (9), L well spaced out points in the interior of Ω are selected. These points are denoted by $(x_1^{(2N+1)}, x_2^{(2N+1)}), (x_1^{(2N+2)}, x_2^{(2N+2)}), \ldots, (x_1^{(2N+L)}, x_2^{(2N+L)})$.

One then approximates the expression $\left[\left[\frac{b(x,y)}{\sqrt{\xi(x,y)}} + p(x,y)\right] w(x,y) - \frac{1}{\sqrt{\xi(x,y)}} f(x,y)\right]$ in (9) using radial basis functions as follows:

$$\left[\left[\frac{b(x,y)}{\sqrt{\xi(x,y)}} + p(x,y)\right] w(x,y) - \frac{1}{\sqrt{\xi(x,y)}} f(x,y)\right] \simeq \sum_{j=1}^{2N+L} \alpha^{(j)} \rho^{(j)}(x,y), \tag{10}$$

where $\alpha^{(j)}$ are unknown parameters to be determined and the radial basis functions $\rho^{(j)}(x,y)$ are given by (for more details see [26]):

$$\rho^{(j)}(x,y) = 1 + \left((x - x_1^{(j)})^2 + (y - x_2^{(j)})^2\right) + \left((x - x_1^{(j)})^2 + (y - x_2^{(j)})^2\right)^{3/2}$$

for $j = 1, 2, \ldots, 2N + L$.

Using (10), the double integral in (9) can now be approximated as

$$\int_\Omega w^*(x,y;\xi,\eta) \left[\left[\frac{\gamma(x,y)}{\sqrt{\xi(x,y)}} + p(x,y)\right] w(x,y) - \frac{1}{\sqrt{\xi(x,y)}} f(x,y)\right] dx\, dy \simeq \sum_{j=1}^{2N+L} \mu^{(kj)} \Psi^{(j)}(\xi,\eta), \tag{11}$$

where

$$\Psi^{(j)}(\xi,\eta)=\lambda(\xi,\eta)\chi^{(j)}(\xi,\eta)+\int_{\partial\Omega}\left(w^*(x,y;\xi,\eta)\frac{\partial\chi^{(j)}}{\partial n}(x,y)-\chi^{(j)}\frac{\partial w^*}{\partial n}(x,y;\xi,\eta)\right)ds(x,y)$$

and

$$\chi^{(j)}\big(x,y;x_1^{(j)},x_2^{(j)}\big)=\frac{1}{4}\big((x-x_1^{(j)})^2+(y-x_2^{(j)})^2\big)+\frac{1}{16}\big((x-x_1^{(j)})^2+(y-x_2^{(j)})^2\big)^2+\frac{1}{25}\big((x-x_1^{(j)})^2+(y-x_2^{(j)})^2\big)^{\frac{5}{2}}.$$

The function $\Psi^{(j)}(\xi,\eta)$ can be computed approximately using

$$\Psi^{(j)}(\xi,\eta)=\lambda(\xi,\eta)\chi^{(j)}(\xi,\eta)+\sum_{m=1}^{N}\chi^{(j)}\big(x_1^{(m)},x_2^{(m)}\big)I_1^{(m)}(\xi,\eta)+\chi^{(j)}\big(x_1^{(N+m)},x_2^{(N+m)}\big)I_2^{(m)}(\xi,\eta)-\frac{\partial\chi^{(j)}}{\partial n}\big(x_1^{(m)},x_2^{(m)}\big)I_3^{(m)}(\xi,\eta)-\frac{\partial\chi^{(j)}}{\partial n}\big(x_1^{(N+m)},x_2^{(N+m)}\big)I_4^{(m)}(\xi,\eta).$$

Then letting (ξ,η) in (9) and (11) be given by $(\xi,\eta)=(x_1^{(n)},x_2^{(n)})$ for $n=1,2,\dots,2N+L$, one finds that

$$\begin{aligned}\lambda\big(x_1^{(n)},x_2^{(n)}\big)w^{(n)}=&\sum_{k=1}^{2N+L}\left[\left[\frac{b\big(x_1^{(k)},x_2^{(k)}\big)}{\sqrt{\xi(x_1^{(k)},x_2^{(k)})}}+p\big(x_1^{(k)},x_2^{(k)}\big)\right]w^{(k)}-\frac{1}{\sqrt{\xi(x_1^{(k)},x_2^{(k)})}}f\big(x_1^{(k)},x_2^{(k)}\big)\right]\\&\times\sum_{j=1}^{2N+L}\mu^{(kj)}\Psi^{(j)}\big(x_1^{(n)},x_2^{(n)}\big)+\sum_{m=1}^{N}\Big(w^{(m)}I_1^{(m)}\big(x_1^{(n)},x_2^{(n)}\big)+w^{(N+m)}I_3^{(m)}\big(x_1^{(n)},x_2^{(n)}\big)\Big)\\&-\sum_{m=1}^{N}\left(\frac{\partial w^{(m)}}{\partial n}I_2^{(m)}\big(x_1^{(n)},x_2^{(n)}\big)+\frac{\partial w^{(N+m)}}{\partial n}I_4^{(m)}\big(x_1^{(n)},x_2^{(n)}\big)\right).\end{aligned}$$

We may use the substitution (6) in order to derive the following:

$$\begin{aligned}\lambda\big(x_1^{(n)},x_2^{(n)}\big)\sqrt{\xi^{(n)}}u^{(n)}=&\sum_{k=1}^{2N+L}\left[\left[\frac{b\big(x_1^{(k)},x_2^{(k)}\big)}{\sqrt{\xi(x_1^{(k)},x_2^{(k)})}}+p\big(x_1^{(k)},x_2^{(k)}\big)\right]w^{(k)}-\frac{1}{\sqrt{\xi(x_1^{(k)},x_2^{(k)})}}f(x_1^{(k)},x_2^{(k)})\right]\\&\times\sum_{j=1}^{2N+L}\mu^{(kj)}\Psi^{(j)}(x_1^{(n)},x_2^{(n)})\\&+\sum_{m=1}^{N}\left(\sqrt{\xi^{(m)}}u^{(m)}I_1^{(m)}\big(x_1^{(n)},x_2^{(n)}\big)+\sqrt{\xi^{(N+m)}}u^{(N+m)}I_3^{(m)}\big(x_1^{(n)},x_2^{(n)}\big)\right)\\&-\sum_{m=1}^{N}\left(\xi^{(m)}\frac{\partial u^{(m)}}{\partial n}+u^{(m)}\frac{\partial\xi^{(m)}}{\partial n}\right)I_2^{(m)}\big(x_1^{(n)},x_2^{(n)}\big)\\&+\left(\xi^{(N+m)}\frac{\partial u^{(N+m)}}{\partial n}+u^{(N+m)}\frac{\partial\xi^{(N+m)}}{\partial n}\right)I_4^{(m)}\big(x_1^{(n)},x_2^{(n)}\big),\end{aligned}$$

where $u^{(m)}=u\big(x_1^{(m)},x_2^{(m)}\big)$ with $m=1,2,\dots,2N+L$. By applying the boundary conditions either $u^{(m)}$ or $\frac{\partial u^{(N+m)}}{\partial n}$ (not both) is known for $m=1,2,\dots,2N$. In addition of the L unknown in the interior of the domain, roughly speaking we get the following matrix system:

$$AX=B. \tag{12}$$

Which can be solved for $2N+L$ unknowns given by $u^{(m)}$ or $\frac{\partial u^{(m)}}{\partial n}$ for $m=1,2,\dots,2N$ and $u^{(2N+k)}$ for $k=1,\dots,L$.

4.2. Regularized reconstruction algorithm

Since we are concerned with a gradient-type approach, we have to derive the sensitivity problem. As noted above, the optimization problem (5) is nonlinear with respect to the still unknown γ, this yields to the non-convexity of the optimization problem which makes the resolution more difficult. First, we try to linearize the optimization problem (5), we let a direction $d \in L^\infty(\Gamma_R)$ and we assume that the following lemma holds.

Lemma 2. *The $u(\gamma)$ is differentiable with respect to $\gamma \in \gamma_{ad}$ where we have:*

$$\frac{\|u(\gamma+d)-u(\gamma)-u'(\gamma)d\|_{H^1(\Omega)}}{\|d\|_{L^\infty(\Gamma_R)}} \to 0 \quad as \quad \|d\|_{L^\infty(\Gamma_R)} \to 0.$$

Using lemma (2) we can write:

$$u(\gamma+d) = u(\gamma) + u'(\gamma)d + \mathcal{O}\big(\|d\|^2_{L^\infty(\Gamma_R)}\big).$$

It is standard to see that $\zeta_d = u'(\gamma)d$ verifies the following system:

$$\begin{cases} -\nabla\cdot(\xi(\mathrm{x})\nabla\zeta_d) + b(\mathrm{x})\zeta_d = 0 & \text{in } \Omega, \\ \xi(\mathrm{x})\dfrac{\partial\zeta_d}{\partial n} = 0 & \text{on } \Gamma_N, \\ \xi(\mathrm{x})\dfrac{\partial\zeta_d}{\partial n} + \gamma(\mathrm{x})\zeta_d(\mathrm{x}) = -du(\gamma)(\mathrm{x}) & \text{on } \Gamma_R. \end{cases} \tag{13}$$

Where we neglect the second order term $\mathcal{O}\big(\|d\|^2_{L^\infty(\Gamma_R)}\big)$, obviously the solution of the sensitivity problem (13) is linear with respect to d. For an efficient evaluation of the gradient we need also to derive the adjoint problem of (13), which can be stated as follows:

$$\begin{cases} -\nabla\cdot(\xi(\mathrm{x})\nabla\zeta_p^*) + b(\mathrm{x})\zeta_p^* = 0 & \text{in } \Omega, \\ \xi(\mathrm{x})\dfrac{\partial\zeta_p^*}{\partial n} = p(\mathrm{x}) & \text{on } \Gamma_N, \\ \xi(\mathrm{x})\dfrac{\partial\zeta_p^*}{\partial n} + \gamma(\mathrm{x})\zeta_p^*(\mathrm{x}) = 0 & \text{on } \Gamma_R, \end{cases} \tag{14}$$

Where we have $\zeta_p^* = u'(\gamma)^* p$ and the direction $p = \mathbb{F}(\gamma) - \tilde{u}_\delta$.

We have the following result.

Theorem 4. *For any $\gamma \in \gamma_{ad}$ the objective function $J(\gamma)$ defined in (5) is Frechet differentiable, its Frechet derivative in the direction d is given as follows:*

$$J'(\gamma)d = \int_{\Gamma_R} d\left(u(\gamma)\zeta_p^* + \alpha\gamma\right) ds.$$

Proof. As a first step we derive the Frechet derivative of the objective function J with $\alpha = 0$ noted $J_0'(\gamma)d$ with d is a direction, therefore we can easily find the following result:

$$J_0'(\gamma)d = \int_{\Gamma_N} \left(\mathbb{F}(\gamma) - \tilde{u}_\delta\right)\zeta_d\, ds.$$

Indeed, it is straightforward to derive:

$$\begin{aligned} J_0(\gamma+d) - J_0(\gamma) &= \frac{1}{2}\int_{\Gamma_N} \left(\mathbb{F}(\gamma+d) - \tilde{u}_\delta\right)^2 ds - \frac{1}{2}\int_{\Gamma_N} \left(\mathbb{F}(\gamma) - \tilde{u}_\delta\right)^2 ds \\ &= \int_{\Gamma_N} \Big(\mathbb{F}(\gamma) + \zeta_d + \mathcal{O}\big(\|d\|^2_{L^\infty(\Gamma_R)}\big) - \tilde{u}_\delta\Big)^2 ds - \int_{\Gamma_N} \left(\mathbb{F}(\gamma) - \tilde{u}_\delta\right)^2 ds \\ &= \int_{\Gamma_N} \left(\mathbb{F}(\gamma) - \tilde{u}_\delta\right)\zeta_d\, ds + \mathcal{O}\big(\|d\|^2_{L^\infty(\Gamma_R)}\big), \end{aligned}$$

thus we have the result.

On the other hand, using Green's second identity after multiplying the problem (13) by ζ_p^* and the problem (14) by ζ_d, we get by substituting the boundary condition:

$$\int_{\Gamma_N} (\mathbb{F}(\gamma) - \tilde{u}_\delta)\, \zeta_d \, ds = \int_{\Gamma_R} du(\gamma)\zeta_p^* \, ds,$$

which completes the proof. ∎

In the next two paragraphs, we propose two automatic regularizing algorithms for the reconstruction of the Robin coefficient.

4.3. Regularized BFGS quasi-Newton algorithm for Robin coefficient recovery

In the present study, we first present a well-known Newton-type method to retrieve the unknown Robin parameter, since this method requires the evaluation of the Hessian matrix which is computationally expensive, we prefer to use a Secant method. It involves the use of a cheaper approximation of the Hessian matrix, practically the best update choice is the Broyden–Fletcher–Goldfarb–Shanno (BFGS) quasi-Newton algorithm [27–30] formula.

The quasi-Newton process iteratively produces a sequence of solutions γ_k by the line search formula

$$\gamma_{k+1} = \gamma_k + \beta_k d^k,$$

with β_k is the step length parameter, whereas the line search direction is obtained using the formula:

$$d^k = M_k E_k,$$

E_k denotes the gradient, and M_k is the approximate inverse of the Hessian matrix, it must be noted that the given initial M^0 should be positive definite and that the update M^k verifies the following condition:

$$M^{k+1}(E^{k+1} - E^k) = \gamma_{k+1} - \gamma_k.$$

We can now describe the quasi-Newton automatic regularization BFGS.

Algorithm 1 The regularized BFGS-DDM for Robin coefficient reconstruction.

Require: Set $k = 0$ and specify the initial guess γ_0 and the initial reduced hessian matrix $M^0 = I$.

1. **Compute** $\mathbb{F}(\gamma_k)$ and **Calculate** $r_k = \mathbb{F}(\gamma_k) - \tilde{u}_\delta$ on Γ_N.
2. **Find** ζ_p^* by solving (14) with $p = r_k$.
3. **Determine** the gradient $E^k = J'(\gamma_k)$ using Theorem (4).
4. **Find** $\beta^k = \arg\min(J(\gamma_k + \beta d^k))$ from a line search, with $d^0 = -E^0$.
5. **Update Robin coefficient:**
$$\gamma_{k+1} = \gamma_k + \beta^k d^k.$$
6. **The discrepancy stopping criterion:**
$$r_{k+1} = \|\mathbb{F}(\gamma_{k+1}) - \tilde{u}_\delta\|_{L^2(\Gamma_N)} \leqslant c\delta$$
does not hold then **Stop**; **Output** γ_k.
7. **Evaluate** $W^k = E^{k+1} - E^k$.
8. **Update** reduced Hessian matrix using
$$M^{k+1} = \left(I - \frac{d^k W^{kT}}{d^{kT} W^k}\right) M^k \left(I - \frac{W^k d^{kT}}{d^{kT} W^k}\right) + \frac{d^k d^{kT}}{d^{kT} W^k}.$$
9. **Evaluate** $d^{k+1} = M^{k+1} W^k$ and return to 2 with $k := k + 1$.

We noticed that the algorithm 1 consists of a combination of an inner and outer iterations, where the BFGS quasi-Newton algorithm is the inner iteration that tries to find a regularized approximation to the linearized problem, whereas the outer iteration terminates the iteration procedure at the right index.

4.4. Automated Levenberg-Marquardt algorithm for Robin coefficient recovery

In addition to the previous algorithm, we propose to minimize the cost functional through an iterative regularized Levenberg–Marquardt algorithm [32], which is given as follows:

$$\gamma_{n+1} = \underset{\gamma\in\gamma_{ad}}{\arg\min} \left\|u'(\gamma_n)(\gamma-\gamma_n) - y - u(\gamma_n)\right\|^2_{L^2(\Gamma_N)} + \alpha_n\|\gamma-\gamma_n\|^2_{L^2(\Gamma_R)}.$$

This equivalently leads to the following:

$$\gamma_{n+1} = \gamma_n + \left(\alpha_n I + u'(\gamma_n)^* u'(\gamma_n)\right)^{-1} u'(\gamma_n)^* \left(u(\gamma_n) - \tilde{u}_\delta\right). \tag{15}$$

Instead of a fixed regularizing parameter, the iterative Levenberg–Marquardt algorithm tries to stabilize the reconstruction procedure in each iteration, one has to note that in case of noisy measurements, which is the case in this study, a stopping criterion has to be carried out, in other words, the iteration process has to be stopped in the right index to obtain a stable solution. In this paper the parameters α_n are chosen according to Morozov discrepancy principle.

The regularizing property of the iterated Levenberg–Marquardt method was well established in [31], the author claimed that if we assume the local boundedness of $\mathbb{F}'$ and that the parameters α_n are chosen via Morozov discrepancy principle and a well-chosen initial guess, we have $\gamma_{K_\delta} \to \gamma^*$ as $\delta \to 0$ with $K_\delta = K(\delta, \tilde{u}_\delta)$ is the stopping index. For a complete study of the convergence of the Levenberg-Marquardt algorithm please see [31].

At this stage, we may outline the automatic regularizing Levenberg–Marqwardt algorithm with the discontinuous dual reciprocity approximation (LM-DDM) for retrieving the yet unknown Robin coefficient:

Algorithm 2 The automated regularizing LM-DDM for Robin coefficient reconstruction.

Require: Set $k = 0$ and specify $\alpha_0 \geqslant 0$, the initial guess γ_0 and a constant $c \geqslant 1$.

1. **Compute** the matrix $A(\gamma_k)$ issued from the DDM in (12).
2. **Compute** the second member $B(\gamma_k)$.
3. **Solve** $A\mathbb{F}(\gamma_k) = B(\gamma_k)$ using LU decomposition.
4. **Solve** $LU\mathbb{F}(\gamma_k) = B(\gamma_k)$.
5. **Compute** $\mathbb{F}'(\gamma_k)$ and $\mathbb{F}' * (\gamma_k)$ using (13) and (14) respectively.
6. **Compute** the next iteration γ_{k+1} using (15)
7. **The stopping criterion** $Res_{k+1} = \|\mathbb{F}(\gamma_{k+1}) - \tilde{u}_\delta\|_{L^2(\Gamma_N)} \leqslant c\delta$ doesn't hold
   then **Stop**; **Output** γ_k.
8. **Update** α_k
   if $(Res_{k+1} \geqslant Res_k)$ then **update** $\alpha_{k+1} = 0.1\alpha_k$;
   else $\alpha_{k+1} = 10\alpha_k$.
9. **Return to** 1 with $k := k + 1$.

It must be noted that in the algorithm 2, the Frechet derivative is applied only to a single argument, which makes the computation cost much cheaper than constructing then reversing the whole derivative matrix which is usually dense. Contrary to the previous algorithm, the inner iteration here is applying the Levenberg–Marquardt algorithm to the linearized problem with some automatic choice of the damping parameter, which theoretically guarantees the stability of the algorithm together with the stopping criteria based on the Discrepancy principle.

5. Numerical experiments

In order to test the proposed numerical approaches for some numerical examples, we examine the case of exact and noisy data for different types of geometries, namely, regular and piecewise regular geometries. We consider the following elliptic problem for anisotropic nonhomogeneous materials:

$$\begin{cases} -\nabla \cdot (\xi(\mathrm{x})\nabla u) + b(\mathrm{x})u = f(\mathrm{x}) & \text{in } \Omega, \\ u = g(\mathrm{x}) & \text{on } \Gamma_D, \\ \xi(\mathrm{x})\dfrac{\partial u}{\partial n} = h(\mathrm{x}) & \text{on } \Gamma_N, \\ \xi(\mathrm{x})\dfrac{\partial u}{\partial n} + \gamma(\mathrm{x})u(\mathrm{x}) = k(\mathrm{x}) & \text{on } \Gamma_R. \end{cases} \tag{16}$$

As outlined above, we try to retrieve the Robin coefficient γ using some additional measurements on the accessible part Γ_N, supposed to be exact and perturbed in two essential cases of domains. The perturbation of the measurements data are simulated using the following formula:

$$\tilde{u}_\delta = \tilde{u} + \delta \times randn \times \|\tilde{u}\|_\infty, \tag{17}$$

where $randn$ is a random scalar drawn from the standard normal distribution and δ represents the level of noise added to the input data.

5.1. Case 1: Regular

In this part, we aim to evaluate the LM-DDM 2 and BFGS-DDM 1 algorithms for reconstructing Robin coefficient in regular domains (the unit circle), we investigate the use of exact and noisy data. The analytical quantities used in implementation are given as follows:

$$u_{an} = \exp(x+y), \quad \xi_{an} = 1, \quad b = 1, \quad \gamma_{an} = 1 + \cos(\pi/4x)\sin(\pi/4y).$$

5.1.1. Exact measurements

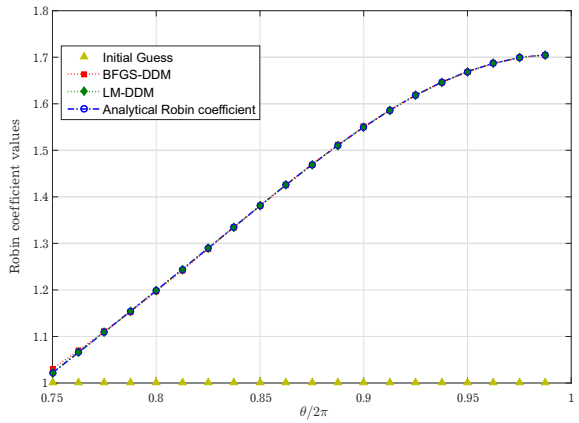

Fig. 1. LM-DDM for Robin coefficient identification with exact data case 1.

When exact data on the accessible part of the boundary are provided, we notice easily that the LM-DDM algorithm recovers much better the Robin coefficient than the BFGS-DDM, as illustrated in Figure 1. The starting guess if given as $\gamma_0 = 1$, some other tests, not presented in this study, confirm that the proposed approach has the ability to recover the Robin coefficient even with a far initial guess, the only difference is the augmentation of the number of iterations, we note that in the free data case the stopping criteria is chosen as the residual reaches a certain tolerance given by 1e-6.

5.1.2. Perturbed measurements

The stability issue can only be investigated in case of perturbed data. Using formula (17), we simulate the noisy effect, the noise level is chosen between $\{1\%, \ldots, 5\%\}$. The performance of the algorithms is clearly influenced by the augmentation of the noise level, especially when $\delta = 5\%$, but the results, in

general, are very promising: when the noise is lower than 1%, the results show that the algorithms are stable enough with slight superiority of the LM-DDM algorithm, this is mainly due to the damping parameter involved in the Levenberg–Marquardt formula that has a stabilizing effect.

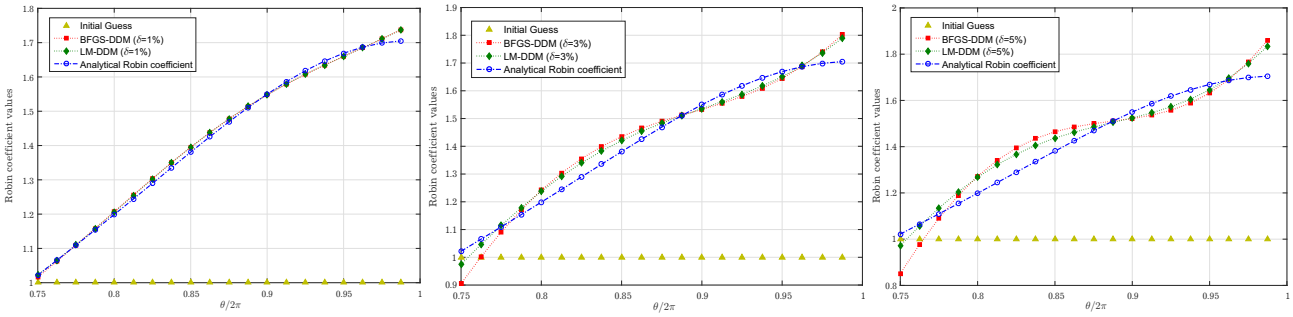

a $(\delta = 1\%)$ ***b*** $(\delta = 3\%)$ ***c*** $(\delta = 5\%)$

Fig. 2. LM-DDM and BFGS-DDM for Robin coefficient identification with noisy data, case 1.

5.2. Case 2: Piecewise regular

In this part, we investigate another class of domain problem, namely, the piecewise regular domain (a traditional choice is the unit square). Similarly, we try to see how the proposed algorithms 1 and 2 perform in this case. We try a different example where the analytical quantities used in implementation are given as follows:

$$u_{an} = \cos(x+y), \quad \xi_{an} = \exp(-x-y), \quad b = 2xy, \quad \gamma_{an} = 2 + \sin(3\pi/y).$$

5.2.1. Exact measurements

Figure 3 presents the obtained results using exact measurements, the optimal solution coincides perfectly with the analytical solution and we note that this can only validate the reconstruction process of the proposed approach.

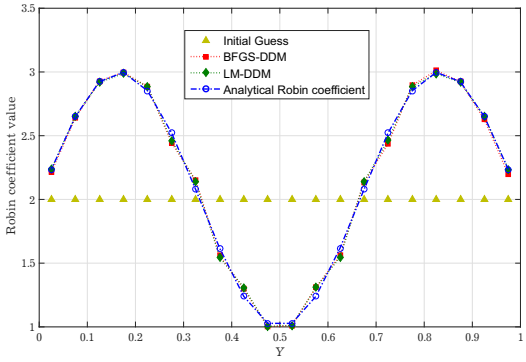

Fig. 3. LM-DDM for Robin coefficient identification with exact data case 2.

5.2.2. Perturbed measurements

The stability performance is again studied in this case, crucially Figure 4 attests that the LM-DDM algorithm performs well in case of the piecewise regular domain, but, for a bigger δ the algorithm performs below expectations. It must be noted that the results are very promising for a lower percentage of δ, and the fact that the discontinuous reciprocity approximation is effective for this kind of domains.

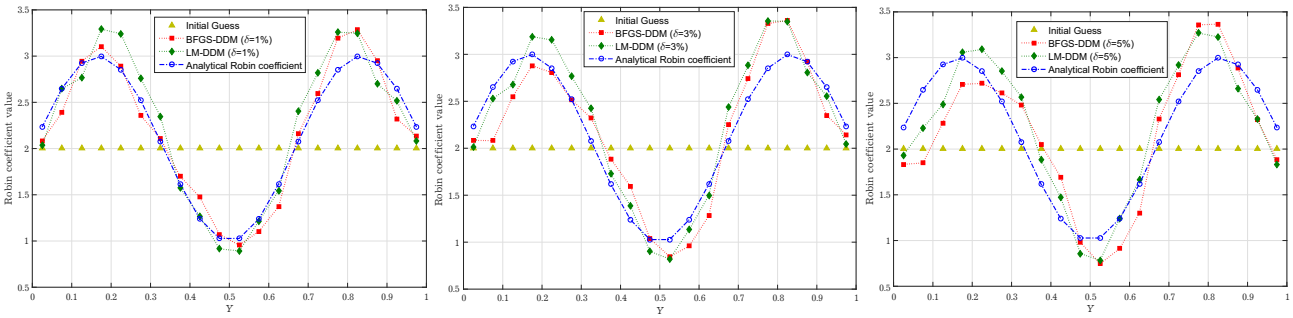

a $(\delta = 1\%)$ ***b*** $(\delta = 3\%)$ ***c*** $(\delta = 5\%)$

Fig. 4. LM-DDM and BFGS-DDM for Robin coefficient identification with noisy data, case 2

6. Conclusions

In this study, two stable strategies are presented to recover an unknown Robin coefficient in a 2D elliptic equation for anisotropic nonhomogeneous domains, a standard mathematical analysis of the present inverse problem is carried out, and many numerical tests are given to confirm the theoretical finds. The LM-DDM algorithm has proved slight superiority in comparison with the BFGS-DDM algorithm in terms of accurateness and speed, in general, the two approaches have revealed their effectiveness in accurately recovering the Robin coefficient for different geometries, the stability is also tested by simulating the noisy effect in provided data. The most striking point in the present work is when a higher noise level is considered, future work will be more interested in this unexpected drawback.

[1] Chantasiriwan S. Inverse heat conduction problem of determining time-dependent heat transfer coefficient. International Journal of Heat and Mass Transfer. **42** (23), 4275–4285 (1999).

[2] Divo E., Kassab A. J., Kapat J. S., Chyu M.-K. Retrieval of multi dimensional heat transfer coefficient distributions using an inverse BEM-based regularized algorithm: numerical and experimental results. Engineering Analysis with Boundary Elements. **29** (2), 150–160 (2005).

[3] Inglese G. An inverse problem in corrosion detection. Inverse Problems. **13** (4), 977–994 (1997).

[4] Alessandrini G., Piero L. D., Rondi L. Stable determination of corrosion by a single electrostatic boundary measurement. Inverse Problems. **19** (4), 973–984 (2003).

[5] Fang W., Cumberbatch E. Inverse problems for metal oxide semiconductor field-effect transistor contact resistivity. SIAM Journal on Applied Mathematics. **52** (3), 699–709 (1992).

[6] Beck J. V., Osman A. M. Inverse problem for the estimation of time-and-space dependent heat transfer coefficients. Journal of Thermophysics and Heat Transfer. **3** (2), 146–152 (1989).

[7] Kaup P. G., Santosa F. Nondestructive evaluation of corrosion damage using electrostatic measurements. Journal of Nondestructive Evaluation. **14** (3), 127–136 (1995).

[8] Chaabane S., Jaoua M. Identification of Robin coefficients by the means of boundary measurements. Inverse Problems. **15** (6), 1425–1438 (1999).

[9] Choulli M. An inverse problem in corrosion detection: Stability estimates. Journal of Inverse and Ill-Posed Problems. **12** (4), 349–367 (2004).

[10] Sinsich E. Lipschitz stability for the inverse Robin problem. Inverse Problems. **23** (3), 1311–1326 (2007).

[11] Alessandrini G., Piero L. D., Rondi L. Stable determination of corrosion by a single electrostatic boundary measurement. Inverse problems. **19** (4), 973–984 (2003).

[12] Chaabane S., Fellah I., Jaoua M., Leblond J. Logarithmic stability estimates for a Robin coefficient in 2D Laplace inverse problems. Inverse Problems. **20** (1), 47–59 (2004).

[13] Leblond J., Mahjoub M., Partington J. R. Analytic extensions and Cauchy-type inverse problems on annular domains: stability results. Journal of Inverse and Ill-Posed Problems. **14** (2), 189–204 (2006).

[14] Alessandrini G., Sincih E. Detection of nonlinear corrosion by electrostatic measurements. Applicable Analysis. **85** (1–3), 107–128 (2006).

[15] Kabanikhin S. I., Karchevsky A. L. Optimizational method for solving the Cauchy problem for an elliptic equation. Journal of Inverse and Ill-Posed Problems. **3** (1), 21–26 (1995).

[16] Slodiscka M., Vankeer R. Determination of the convective transfer coefficient in elliptic problems from a nonstandard boundary condition. In: J. Maryska, M. Tuma, J. Sembera (eds) Simulation, modelling, and numerical analysis, SIMONA 2000. 13–20 (2000).

[17] Fasino D., Inglese G. Stability of the solutions of an inverse problem for Laplace's equation in a thin strip. Numerical Functional Analysis and Optimization. **22** (5–6), 549–560 (2001).

[18] Ellabib A., El Madkouri A. A Discontinuous Dual Reciprocity Method in Conjunction with a Regularized Levenberg–Marquardt Method for Source Term Recovery in Inhomogeneous Anisotropic Materials. International Journal of Computational Methods. **17** (10), 2050002 (2020).

[19] El Madkouri A., Ellabib A. A Preconditioned Krylov Subspace Iterative Methods for Inverse Source Problem by Virtue of a Regularizing LM-DRBEM. International Journal of Applied and Computational Mathematics. **6** (4), 94 (2020).

[20] El Madkouri A., Ellabib A. Source term identification with discontinuous dual reciprocity approximation and quasi-Newton method from boundary observations. Journal of Computational Mathematics. **39** (3), 311–332 (2020).

[21] Lions J. L., Magenes E. Non-Homogeneous Boundary Value Problems and Applications. Springer, Berlin (1972).

[22] Isakov V. Inverse source problems. Vol. 34. American Mathematical Soc. (1990).

[23] Partridge P. W., Brebbia C. A., Wrobel L. C. The Dual Reciprocity Boundary Element Method. International Series on Computational Engineering. Springer, Dordrecht (1991).

[24] Ahmedou Bamba S., Ellabib A., El Madkouri A. Simulation of heat distribution in the human eye using discontinuous dual reciprocity boundary element method and non-overlapping domain decomposition approach. Mathematical Modeling and Computing. **7** (1), 1–13 (2020).

[25] Ahmedou Bamba S., Ellabib A., El Madkouri A. Numerical study of optimal control domain decomposition for nonlinear boundary heat in the human eye. Journal of Mathematical Modeling. **8** (3), 219–240 (2020).

[26] Zhang Y., Zhu S. On the choice of interpolation functions used in the dual-reciprocity boundary-element method. Engineering Analysis with Boundary Elements. **13** (4), 387–396 (1994).

[27] Broyden C. G. The convergence of a class of double-rank minimization algorithms 1. General considerations. IMA Journal of Applied Mathematics. **6** (1), 76–90 (1970).

[28] Fletcher R. A new approach to variable metric algorithms. The Computer Journal. **13** (3), 317–322 (1970).

[29] Goldfarb D. A family of variable-metric methods derived by variational means. Mathematics of Computation. **24** (109), 23–26 (1970).

[30] Shanno D. F. Conditioning of quasi-newton methods for function minimization. Mathematics of Computation. **24** (111), 647–656 (1970).

[31] Hanke M. A regularizing Levenberg–Marquardt scheme, with applications to inverse groundwater filtration problems. Inverse problems. **13** (1), 79–95 (1997).

[32] Fletcher R. Practical methods of optimization. John Wiley & Sons (2013).

Отримання коефіцієнта Робіна з окремих даних Коші в еліптичних системах

Ель Мадкурі А., Еллабіб А.

Факультет наук і техніки,
Кафедра математики та інформатики LAMAI,
Університет Каді Айяда, Марракеш, Марокко

Метою цієї роботи є визначення коефіцієнта Робіна за наявними вимірюваннями на доступній частині границі. Після перетворення оберненої задачі на задачу оптимізації досліджуються питання визначеності, стійкості та ідентифікації. Для процесу реконструкції розроблено два регуляризованих алгоритми, а пряма задача апроксимується за допомогою розривного методу подвійної взаємності. Точність запропонованих підходів перевірена для випадку зашумлених даних та даних без шуму, отримані результати є дуже перспективними та обнадійливими.

Ключові слова: *метод граничних елементів, розривна апроксимація взаємності, алгоритм Левенберга–Марквардта, квазі-алгоритми Ньютона, реконструкція параметрів Робіна.*